EPJ manuscript No.
(will be inserted by the editor)

Energy and System-size Dependence of Two-particle Azimuthal Correlations of High-p_T Charged Hadrons at the CERN SPS

Marek Szuba[a] for the NA49 Collaboration

Faculty of Physics, Warsaw University of Technology, Koszykowa 75, 00-662 Warszawa, Poland

Received: date / Revised version: date

Abstract. Angular correlations of high-p_T hadrons can serve as a probe of interactions of partons with the dense medium produced in high-energy heavy-ion collisions but other sources of such correlations exist which can be non-negligible SPS energies. In an attempt to determine the primary source, NA49 has performed an energy and system-size scan of two-particle azimuthal correlations in central $Pb+Pb$, $Si+Si$ and $p+p$ collisions at 158A GeV, as well as central $Pb+Pb$ collisions at 20A, 30A, 40A and 80A GeV. Moreover, results at 158A GeV have been compared to UrQMD simulations.

PACS. 25.75.Bh Hard scattering in relativistic heavy ion collisions – 25.75.Gz Particle correlations and fluctuations – 25.75.Nq Quark deconfinement, quark-gluon plasma production and phase transitions in relativistic heavy-ion collisions

arXiv:0809.5210v1 [nucl-ex] 30 Sep 2008

1 Introduction

It is believed that one of the signatures of a hot, dense medium expected to appear in most central high-energy collisions of heavy ions, will be modification of properties of jets — highly collimated showers of particles, originating from hard scattering of partons and therefore produced early in a collision — as a result of their interaction with that medium [1]. Unfortunately, direct reconstruction of jets in the presence of a large background typical of such events is an extremely challenging task. One possible answer to this problem is studying two-particle azimuthal correlations, which allow one to extract the jet signal from the soft background by taking advantage of the fact jet particles are strongly correlated in azimuth. In recent years RHIC experiments have made this approach highly successful by not only observing the expected signatures, but also providing, through further investigations, evidence which has led to unexpected conclusions regarding the properties of the hot medium (the "perfect liquid" description; see *e.g.* [2], [3]). However, until recently ([4], [5]) no analyses of this sort were performed in the energy range of the CERN SPS.

What makes investigating hard processes challenging, even with the aid of correlations, in the energy range of the SPS is that their contribution to particle production there is very low, *i.e.* only about 2 percent. Moreover, as SPS-energy collisions do not produce really high-p_T particles it is necessary to perform such analyses in the intermediate region just above 2 GeV/c in which the share of particles originating from soft processes is still non-negligible. Finally, operating in this transverse-momentum region in nucleus-nucleus collisions makes the analysis sensitive to Cronin enhancement, an effect of undetermined origin and thus unknown magnitude. All of the above, together with high uncertainties of pQCD calculations for such low momenta, make it unclear how much of the correlation signal will come from jets and how much from other sources, such as resonances, global momentum conservation etc.

2 Experimental Setup

The NA49 detector is a large-acceptance spectrometer dedicated to the study of hadron production in fixed-target nucleon-nucleon, nucleon-nucleus and nucleus-nucleus collisions at a wide range of energies offered by the CERN SPS. During its eight years of running it has been used to register Pb+Pb collisions at 20A, 30A, 40A, 80A and 158A GeV, $C+C$ and $Si+Si$ collisions at 40A and 158A GeV, along with $p+p$ and $p+Pb$ interactions at 158 GeV.

The main components of the detector are four time projection chambers, used for tracking as well as particle identification by dE/dx. Two of the chambers, the so-called Vertex TPCs, are located inside two superconducting magnets (with field intensity of 1.5 and 1.1 T, respectively) positioned along the beam axis right downstream of the target, with the other two ("Main" TPCs) placed further downstream on both sides of the beam line. Two Time of Flight walls located beyond the MTPCs complement particle identification in the intersection region of Bethe-Bloch dE/dx bands of different particle species. Centrality selection in nucleus-nucleus collisions is based on the projectile spectator energy deposited in the Veto

[a] *Marek.Szuba@if.pw.edu.pl*

Calorimeter, located at the downstream end of the experiment.

The present analysis is based on the following data sets recorded by NA49:

- 3×10^6 $Pb + Pb$ collisions, σ/σ_{geom} = 0–23.5 %, at 158A GeV, from the year 2000;
- 265×10^3 $Pb + Pb$ collisions, σ/σ_{geom} = 0–7.2 %, at 80A GeV, from the year 2000;
- 530×10^3 $Pb + Pb$ collisions, σ/σ_{geom} = 0–7.2 %, at 40A GeV, from the year 1999;
- 447×10^3 $Pb + Pb$ collisions, σ/σ_{geom} = 0–7.2 %, at 30A GeV, from the year 2002;
- 369×10^3 $Pb + Pb$ collisions, σ/σ_{geom} = 0–7.2 %, at 20A GeV, from the year 2002;
- 220×10^3 $Si + Si$ collisions, σ/σ_{geom} = 0–12 %, at 158A GeV, from the year 1998;
- 1.7×10^6 $p+p$ collisions (≈90 % inelastic) at 158 GeV, from the year 2000.

3 The Method

In all data sets except $p+p$, which is taken in its entirety, the two-particle azimuthal correlation function is calculated for the event centrality range of 0–5 %. The transverse momentum bins are 2.5 $GeV/c \leq p_T^{trg} \leq 4.0$ GeV/c for trigger particles and 1.0 $GeV/c \leq p_T^{asc} \leq 2.5$ GeV/c for associates.

Following the prescription of the PHENIX Collaboration [6] we define the correlation function as the ratio of two distributions of $\Delta\phi = \phi_{asc} - \phi_{trg}$, where ϕ is the azimuthal angle: $N_{corr}(\Delta\phi)$, in which both particles come from the same event, and $N_{mix}(\Delta\phi)$, in which the trigger and the associate originate from different events. Division by the mixed-event spectrum accounts for non-uniform detector acceptance. Before the ratio is calculated the two distributions are normalised to unity; this is included in the formula in the form of appropriate integrals.

$$C_2(\Delta\phi) = \frac{N_{corr}(\Delta\phi)}{N_{mix}(\Delta\phi)} \frac{\int N_{mix}(\Delta\phi')\mathrm{d}(\Delta\phi')}{\int N_{corr}(\Delta\phi')\mathrm{d}(\Delta\phi')} \qquad (1)$$

In this analysis the mixing is accomplished with a sliding window of up to 50 most recent events in the selected centrality bin.

By default the two distributions, and by extension the correlation function, are presented in the full $\Delta\phi$ range of $\left[-\frac{\pi}{2},\ \frac{3}{2}\pi\right)$. On the other hand, as the correlations under consideration are expected to be symmetric around the back-to-back axis it is possible to reduce statistical errors by folding the function in half[1]. In order to avoid potential normalisation problems the folding is performed on $N_{corr}(\Delta\phi)$ and $N_{mix}(\Delta\phi)$ before they are used in Equation 1; binning of the two distributions was selected to enable an exact bin-by-bin fold from $\left[-\frac{\pi}{2},\ \frac{3}{2}\pi\right)$ to $[0,\ \pi]$.

All results presented here contain statistical errors only. Investigation of systematic uncertainties is ongoing.

[1] Systematic uncertainties introduced by this procedure are being investigated and will be discussed at a later date.

Simulated reference data for the analysis were produced using the string-hadronic model UrQMD [7] [8]. Version 2.3 of the model was used, which among other improvements is the first version of the model to incorporate jet production from PYTHIA [9]. Four data sets of 100,000 events each were produced:

- $Pb+Pb$ collisions at 158A GeV, $b = 0$ fm, jet production enabled;
- $Pb+Pb$ collisions at 158A GeV, $b = 0$ fm, jet production disabled;
- $p+p$ collisions at 158 GeV, $b = 0$ fm, jet production enabled;
- $p+p$ collisions at 158 GeV, $b = 0$ fm, jet production disabled;

4 Results

4.1 System-size Scan

Figure 1 shows two-particle azimuthal correlation functions from $p+p$ and central $Si+Si$ collisions at 158A GeV, compared to those obtained earlier from central lead–lead data at the same energy [5]. Overall strength of the correlation becomes significantly larger as the system size decreases. Moreover, no flattening of the away-side peak, as present in central heavy-ion events, is visible in $Si+Si$ and $p+p$ collisions — indeed, the peak becomes narrower with decreasing system size.

4.2 Energy Scan

In Figure 2 the correlation function from central $Pb+Pb$ collisions at 158A GeV is compared to results from the same system at 80A, 40A, 30A and 20A GeV. The near-side peak appears to turn into depletion with decreasing energy, then again the shape and amplitude of away-side enhancement remains mostly unchanged throughout the scan. Should the flattening of the latter be considered a signature of a hot, dense medium, these results are at odds with present-day expectations that such a medium is produced only at higher energies. On the other hand, the observed away-side enhancement appears to be consistent with global momentum conservation.

4.3 Comparison with UrQMD

A comparison of real-data azimuthal correlation functions from central-$Pb+Pb$ and $p+p$ collisions with results obtained from UrQMD simulations can be found in Figures 3 and 4, respectively. For both systems fairly good agreement can be observed between the data and the simulations, regardless of whether production of jets was enabled in the model or not. These results are again consistent with momentum conservation, however due to the nature of UrQMD it is not possible to say at this point whether it is global or local.

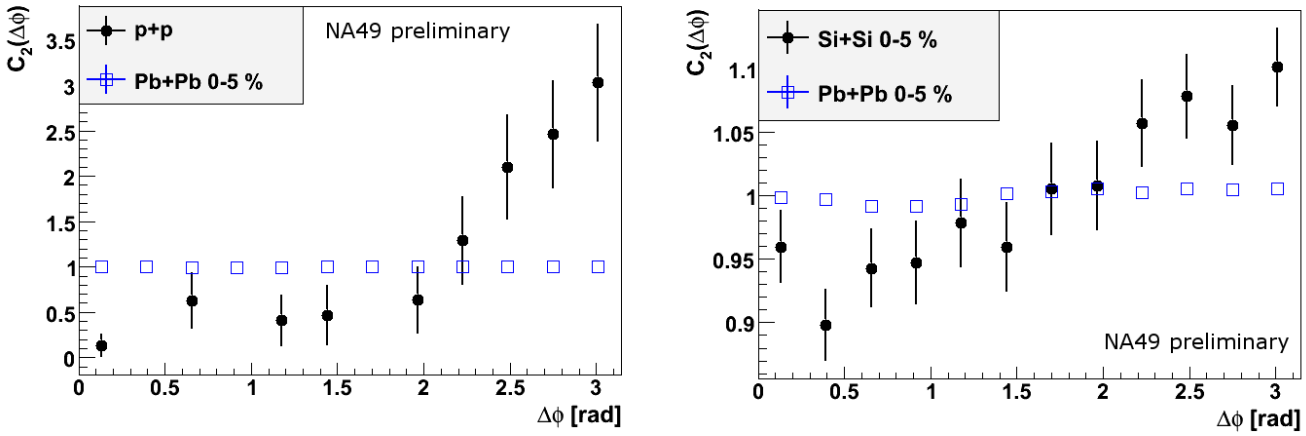

Fig. 1. Two-particle correlation functions from $p + p$ (left) and central $Si + Si$ (right) events at 158A GeV, compared to central-$Pb + Pb$ results at the same energy.

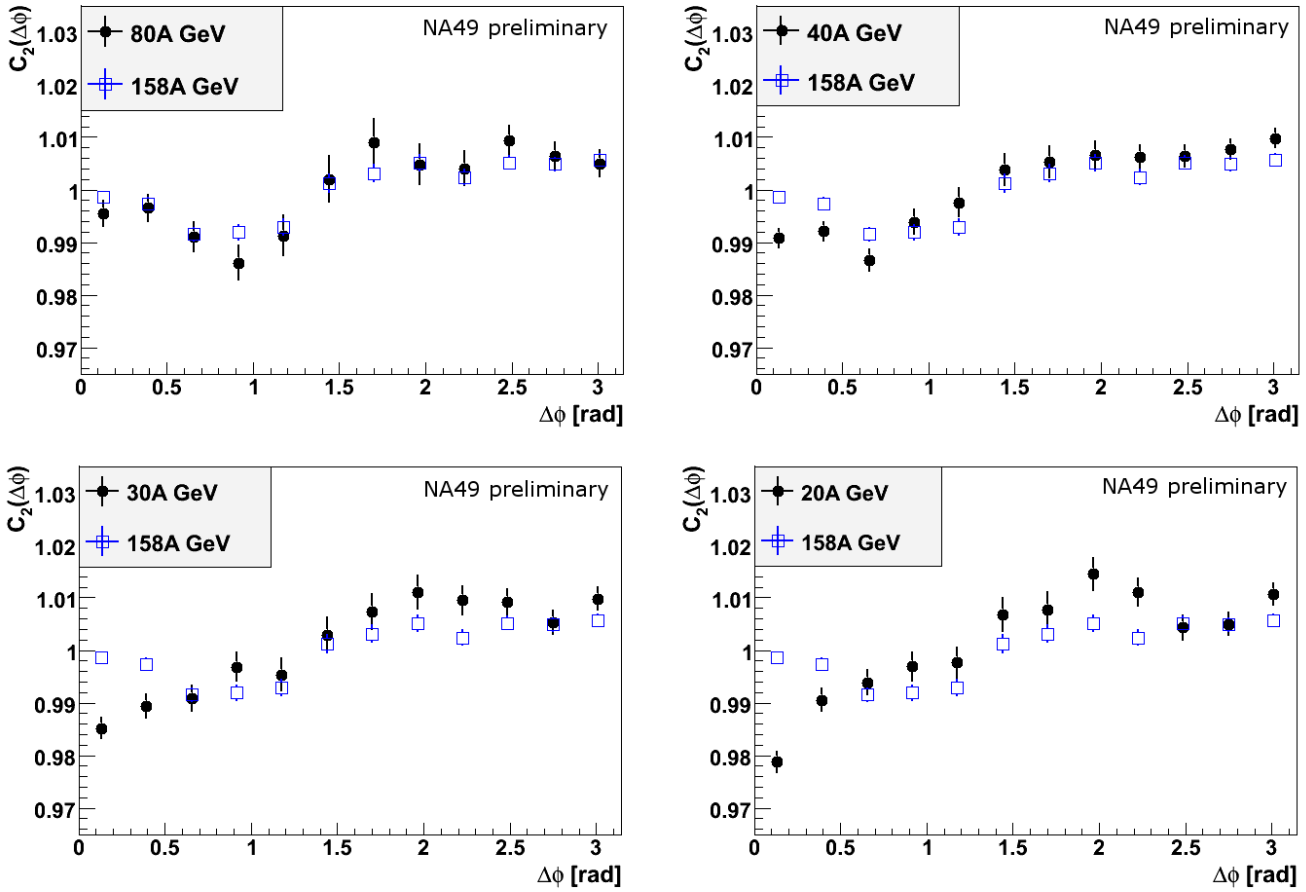

Fig. 2. Two-particle correlation functions from central $Pb + Pb$ events at 80A (top left), 40A (top right), 30A (bottom left) and 20A (bottom right) GeV, compared to results from the same system at 158A GeV.

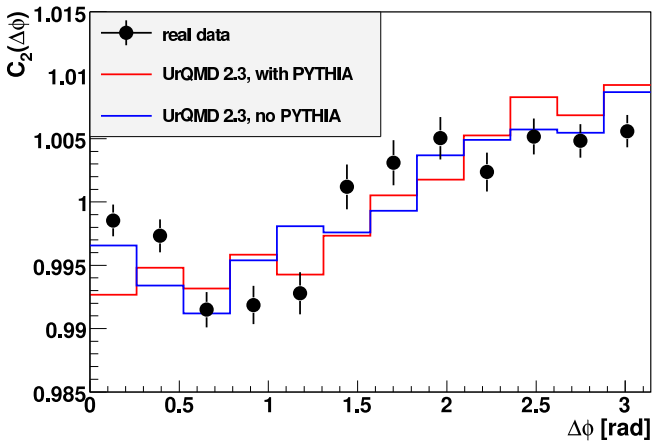

Fig. 3. Comparison of experimental and simulated correlation functions for central lead–lead collisions at 158A GeV. Black points: experimental data, red line: UrQMD with jets, blue line: UrQMD without jets.

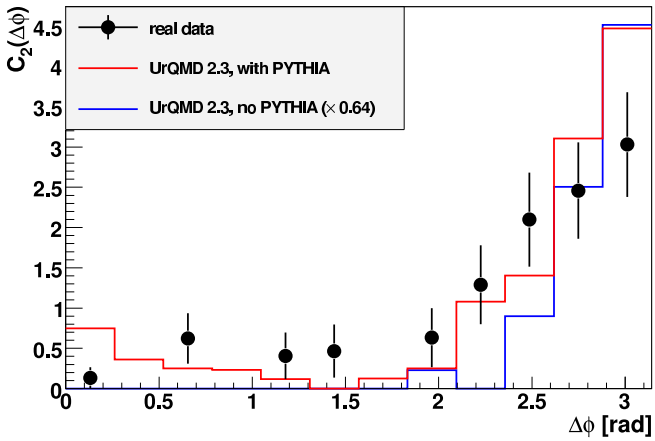

Fig. 4. Comparison of experimental and simulated correlation functions for proton–proton collisions at 158 GeV. Black points: experimental data, red line: UrQMD with jets, blue line: UrQMD without jets (scaled to match the amplitude of the away-side peak of with-jets data).

5 Summary

A system-size and energy scan of two-particle correlation functions from NA49 has been performed. It was found that flattening of the function's away-side peak can be observed in central heavy-ion collisions even at low SPS energies, where no hot, dense medium is expected. On the other hand, all results appear to be consistent with global momentum conservation.

Comparison with results from UrQMD show good agreement between the model and the experiment. Furthermore, the former exhibit little dependence on presence or absence of jets in the sample, favouring the momentum-conservation hypothesis. Further analysis involving statistical models is required in order to determine whether this conservation is global or local.

References

1. X.-N. Wang, M. Gyulassy, Phys. Rev. Lett. **68**, (1992) 1480-1483.
2. J. Adams *et al.* (STAR Collaboration), Phys. Rev. Lett. **95**, (2005) 152301.
3. C. Zhang for the PHENIX Collaboration, J. Phys. G **34**, (2007) S671-S674.
4. M. Ploskon for the CERES Collaboration, Acta Phys. Hung. **A27**, (2006) 255-258.
5. M. Szuba for the NA49 Collaboration, arXiv:0805.4637 [nucl-ex], to be published in Indian Journal of Physics.
6. S.S. Adler *et al.* (PHENIX Collaboration), Phys. Rev. Lett. **97**, (2006) 052301.
7. S.A. Bass, M. Belkacem, M. Bleicher, M. Brandstetter, L. Bravina, C. Ernst, L. Gerland, M. Hofmann, S. Hofmann, J. Konopka, G. Mao, L. Neise, S. Soff, C. Spieles, H. Weber, L.A. Winckelmann, H. Stocker, W. Greiner, Ch. Hartnack, J. Aichelin and N. Amelin, Prog. Part. Nucl. Phys. 41, (1998) 225-370.
8. M. Bleicher, E. Zabrodin, C. Spieles, S.A. Bass, C. Ernst, S. Soff, L. Bravina, M. Belkacem, H. Weber, H. Stocker, W. Greiner, J. Phys. G: Nucl. Part. Phys. 25, (1999) 1859-1896.
9. T. Sjöstrand, S. Mrenna, P. Skands, JHEP 0605, (2006) 026.